EXPERIMENTAL CELL RESEARCH 334 (2015) 270–282

Available online at www.sciencedirect.com

ScienceDirect

journal homepage: www.elsevier.com/locate/yexcr

Research Article

3,4-dihydroxyphenylacetic acid, a microbiota-derived metabolite of quercetin, protects against pancreatic β-cells dysfunction induced by high cholesterol

Catalina Carrasco-Pozo[a,b,*], *Martin Gotteland*[a,c], *Rodrigo L. Castillo*[d], *Chen Chen*[b,**]

[a]*Department of Nutrition, Faculty of Medicine, University of Chile, Chile, Av. Independencia 1027, P.O. Box 8380453 Santiago, Chile*
[b]*School of Biomedical Sciences, The University of Queensland, Brisbane, QLD 4072, Australia*
[c]*Institute of Nutrition and Food Technology, University of Chile, Av. Macul 5540, P.O. Box 138-11, Santiago, Chile*
[d]*Pathophysiology Program, Faculty of Medicine, University of Chile, Av. Independencia 1027, P.O. Box 8380453, Santiago, Chile*

ARTICLE INFORMATION

Article Chronology:
Received 1 January 2015
Received in revised form
22 March 2015
Accepted 26 March 2015
Available online 4 April 2015

Keywords:
3,4 dihydroxyphenylacetic acid
Insulin secretion
ATP
Cholesterol
Mitochondrial dysfunction
Pancreatic β-cell
Superoxide anion radicals

ABSTRACT

Cholesterol plays an important role in inducing pancreatic β-cell dysfunction, characterized by an impaired insulin secretory response to glucose, representing a hallmark of the transition from pre-diabetes to diabetes. 3,4 dihydroxyphenylacetic acid (ES) is a scarcely studied microbiota-derived metabolite of quercetin with antioxidant properties. The aim of this study was to determine the protective effect of ES against apoptosis, mitochondrial dysfunction and oxidative stress induced by cholesterol in Min6 pancreatic β-cells. Cholesterol decreased viability, induced apoptosis and mitochondrial dysfunction by reducing complex I activity, mitochondrial membrane potential, ATP levels and oxygen consumption. Cholesterol promoted oxidative stress by increasing cellular and mitochondrial reactive oxygen species and lipid peroxidation and decreasing antioxidant enzyme activities; in addition, it slightly increased Nrf2 translocation to the nucleus. These events resulted in the impairment of the glucose-induced insulin secretion. ES increased Nrf2 translocation to the nucleus and protected pancreatic β-cells against impaired insulin secretion induced by cholesterol by preventing oxidative stress, apoptosis and mitochondrial dysfunction. Nrf2 activation seems to be involved in the mechanisms underlying the antioxidant protection exerted by ES in addition to preventing the disruption of antioxidant enzymatic defenses. Although additional *in vivo* experiments are required, this metabolite is suggested as a promising drug target for the prevention of the pathological development from a pre-diabetic to a diabetic state.

*Corresponding author at: Department of Nutrition, Faculty of Medicine, University of Chile, Chile, Av. Independencia 1027, P.O. Box 8380453 Santiago, Chile.
**Corresponding author at: School of Biomedical Sciences, The University of Queensland, Brisbane, QLD 4072, Australia.
E-mail addresses: catalinacarrasco@med.uchile.cl (C. Carrasco-Pozo), chen.chen@uq.edu.au (C. Chen).

http://dx.doi.org/10.1016/j.yexcr.2015.03.021
0014-4827/

Introduction

Type 2 diabetes mellitus (T2DM) has become a major health issue worldwide due to its high prevalence and its associated morbidity and mortality. Alteration of pancreatic β-cell function leading to an impaired insulin secretory response to glucose is a hallmark of the transition from the pre-diabetic to the diabetic state [1]. Cholesterol plays an important role in pancreatic β-cell dysfunction. This has been suggested by the observation that β-cells from ATP binding cassette transporter 1 (ABCA1) knockout mice display an increased cellular cholesterol content and an impaired insulin secretion; ABCA1 transporter mediates the reverse cholesterol efflux [2]. This is consistent with a previous observation where liver X receptor b knockout mice (LXRbeta−/−) exhibited β-cell dysfunction; this receptor induces the ABCA1 expression in response to cholesterol [3]. Hao et al. found a direct link between elevated cholesterol and reduced insulin secretion in islets isolated from C57BL/6J mice and in INS-1 rat pancreatic β-cells, the normal secretion of this hormone being restored by cholesterol depletion [4]. The LDL receptor, which facilitates cholesterol uptake, in knockout mice (LDLR−/−) exhibits hypercholesterolemia with elevated islet cholesterol levels and β-cell dysfunction, with impaired glucose tolerance and reduced glucose-stimulated insulin secretion [5]. Interestingly, the loss of ABCG1 expression in β-cells impaired insulin secretion, where ABCG1 acts primarily to regulate the subcellular cholesterol distribution in β-cells; thus a critical role for pancreatic β cell-specific cholesterol homeostasis seems to be involved in insulin secretion as well as in β cell dysfunction in diabetes [6]. Few *in vitro* studies have been carried out to elucidate the underlying mechanism of cholesterol-induced insulin secretion impairment; their results suggest that cholesterol may induce β-cell dysfunction by promoting apoptosis through oxidative stress pathways [7,8], mitochondrial damage [9] and alteration in membrane fluidity [10]. This is particularly interesting since pancreatic β-cells are considered to be particularly susceptible to oxidative stress due to their relatively low antioxidant enzyme content [11]. Thus, molecules with antioxidant and mitochondrial protective properties may represent a promising strategy for preventing and delaying β-cell dysfunction induced by high cholesterol.

The flavonol quercetin (QUE, and QUE-glycosylated) is one of the most abundant polyphenols present in fruits and vegetables [12]. Though many healthy systemic effects in humans have been attributed to QUE, it is barely absorbable in the gastrointestinal tract and as a result, in consequence, it accumulates in the lumen [13]. Colonic microbiota can degrade flavonoids, generating a large number of metabolites that can be absorbed and exert biological effects in the body, such as antioxidant, antimicrobial and anti-inflammatory activities, among others [14]. The major microbial metabolite of QUE and its glycosylated derivatives is ES (homoprotocatechuic acid) [15–22], which also possesses potent antioxidant properties. It has been shown that this compound has the highest free radical scavenging activity among several flavonoid metabolites tested *in vitro*, and that it may reduce plasma lipid peroxidation *in vivo* [23,24]. Interestingly, its antioxidant effects have not been addressed in terms of modulating redox-sensitive transcription factors such as Nrf2. This metabolite is detected in human plasma and urine after the ingestion of a standard diet [25], dietary supplementation with QUE derivatives [26] or flavonoid-rich foodstuffs [27]. Studies into the biological effects of ES beyond its antioxidant activity are limited.

The present study endeavored to determine the *in vitro* protective effect of ES against the loss of cell viability, mitochondrial dysfunction and oxidative stress induced by high cholesterol levels in pancreatic β-cells. This study contributes to explaining the "health-promoting" effects of QUE intake [28–31], in particular against the development of type-2 diabetes, taking into account the low bioavailability of this flavonoid.

Materials and methods

Materials

ES, water-soluble cholesterol, Rhod, DCFD, triphenyltin, 1,1,3,3-tetramethoxypropane were purchased from Sigma (St. Louis, USA). CellTiter 96® AQueous One Solution Cell Proliferation Assay, CytoTox-ONE Homogeneous Membrane Integrity Assay kit and CellTiter-Glo luminescent Cell Viability Assay kit were from Promega (Madison, WI, USA). DHE and Cytochrome c ELISA assay kit was purchased from Invitrogen (Life Technologies, CA, USA). MitoSox™ Red mitochondrial superoxide indicator was obtained from Molecular Probes (Eugene, OR, USA). Caspase-3 Colorimetric Activity Assay Kit and Caspase-9 Colorimetric Activity Assay Kit were purchased from Millipore (Millipore Corporation, Bedford, MA, USA). *In situ* Cell Death Detection Kit, fluorescein) was purchased from Roche (Penzberg, Germany). TBARS assay KIT was obtained from Cayman (Cayman Chemical Company, Ann Arbor, MI, USA). Pierce BCA Protein Assay Kit was purchased from Thermo Scientific (Rockford, IL USA). Rat Ultrasensitive Insulin ELISA kit was from ALPCO (Salem, USA). DMEM, FBS, penicillin, and streptomycin were from GIBCO BRL (Grand Island, NY, USA).

Cell culture Min6 cells [9] were kindly provided by Dr. M Garry (Department of Biochemistry, Monash University, Clayton, Australia) with the approval of Dr. J. Miyazaki (Osaka University, Osaka, Japan) and of Dr. Francisco Pérez (University of Chile). The use of this cell line was previously reported by us in Zhao et al. [9]. Min6 cells (passage 38–48) were cultured in DMEM (25 mM glucose) supplemented with 10% heat-inactivated FBS, 100 IU/ml penicillin, 100 μg/ml streptomycin, and 50 μM β-mercaptoethanol in a humidified atmosphere of 95% air and 5%CO_2. The culture medium was changed three times per week. All the values were normalized in relation to protein concentrations determined by the Pierce BCA Protein Assay Kit. All the experiments were conducted in unsupplemented DMEM media. The present study is mainly based on a previous published work where mitochondrial membrane potential impairment was described as an underlying mechanism of toxicity by cholesterol in pancreatic β-cell [9]. In this study the following experimental conditions were used: 320 μM cholesterol, incubation time of 6 h and Min6 cells, according to a previous work reported by us [9]. Cholesterol: methyl-β-cyclodextrin complex (Sigma catalog no. C4951), a "water-soluble cholesterol" containing 47 mg of cholesterol/g solid according to Certificate of Analysis (molar ratio, 1:6 cholesterol/ methyl-β-cyclodextrin) was used to deliver cholesterol to the cells, as previously described [9,32,33]. Considering that methyl-β-cyclodextrin induces mitochondrial cholesterol depletion from cell membranes at very high concentration (~ 2% or

5 mM) [32,34], a ten times lower concentration of this compound in our experiments.

Cell viability assay

Cell viability was measured through the MTS assay and by LDH quantification [35]. MTS is reduced by cells to a colored formazan that is soluble in DMEM media. LDH is a ubiquitous intracellular enzyme whose leakage is used as a marker of cell membrane damage and cell toxicity. Cells were plated in 96-well plate at a density of 5×10^4 cells/well and after 24 h cells were incubated with 320 μM cholesterol in the absence or in the presence of increasing concentration of ES for 6 h. After the treatments, cell supernatants were collected and the LDH released into the medium was measured using the CytoTox-ONE™, which is based on the conversion of resazurin into fluorescent resorufin (λ_{Ex} 560 nm and λ_{Em} 590 nm). Cell treated with Triton X-100 served as positive control, indicating the maximun LDH release. The RFU of the samples was compared with the RFU of the positive control cells. After washing, the ability of cells to reduce MTS was evaluated by measuring the OD at λ 490 nm, using the CellTiter 96® AQueous Assay according to the manufacturer's instructions. Fluorescence and absorbance were measured using a Multi-Mode Microplate Reader (Synergy HT, BioTek and SunriseTM, Tecan; respectively).

Apoptosis evaluation

Apoptosis was quantitated by measuring the activities of caspase-3 and caspase-9, and through the determination of cytochrome c release. Cells were plated in 6-well plates at a density of 1×10^6 cells/well and, after 24 h, they were incubated with 320 μM cholesterol in the absence or the presence of various concentration of ES for 6 h.

The catalytic activity of caspase-3 and caspase-9 was measured independently by using a commercial colorimetric assay according to the manufacturer's instructions [36,37]. The determination is based on the detection of the chromophore p-nitroanilide at 405 nm after its enzymatic cleavage from the labeled substrate DEVD- or LEHD-p-nitroanilide, respectively. Caspase-3 and -7 use the same artificial substrate (DEVD- p-nitroanilide), but caspase-3 has been described as the major executioner involved in the cleavage phase of apoptosis, since it is more promiscuous than caspase-7 in terms of substrates [38]. Accordingly, in the following paragraphs, only caspase-3 will be referred to. The specific caspase-3 and caspase-9 inhibitors, 0.1 μM Ac-DEVD-CHO and 0.1 μM Ac-LEHD-CHO, were used as enzymatic activity controls, according to the manufacturer's instructions. During the caspase assays, samples from cells treated with 320 μM cholesterol were also incubated for 10 min with Ac-DEVD-CHO or Ac-LEHD-CHO, as controls to confirm the specific induction of the activities of caspase-3 or caspase-9 by cholesterol. Enzyme activity was calculated as μmol of p-nitroanilide released/minute/mg of protein.

Cytochrome c was measured using a Cytochrome c Kit ELISA assay, according to manufacturer's instructions [35].

DNA fragmentation was assessed by terminal deoxynucleotide transferase (TdT)-mediated dUTP nick end-labeling (TUNEL) coupled to FITC fluorescence, using a commercial kit (*In situ* Cell Death Detection Kit, fluorescein, Roche), according to manufacturer's instructions. Cells treated with DNase I (RQ1 RNase-Free DNase, Promega, Madison, WI, USA, Cat. M6101) served as positive controls. Fluorescence was visualized by using a fluorescence microscope (Zeiss, AxioScope A1) equipped with a digital camera (Canon EOS Rebel T3). The mean fluorescence intensity was obtained by using the ImageJ program taking into account the area of the culture under observation according to the magnification. Images were captured in fields with 50% of confluency, based on DAPI staining (0.15 μg/mL).

Mitochondrial function assay

Mitochondrial function was evaluated by measuring MMP using Rhod, a cationic lipophilic fluorochrome (λ_{Ex} 500 nm and λ_{Em} 530 nm) which accumulates in the mitochondrial matrix. Cells were plated in 24-well plates at a density of 2×10^5 cells/well and after 24 h cells were incubated with 320 μM cholesterol in the absence or in the presence of ES for 6 h. After washing, cells were incubated with 1 μg/ml Rhod for 10 min at 37 °C. The specific accumulation of Rhod in the mitochondria was evaluated using as control 3 μM triphenyltin, an inductor of mitochondrial membrane permeability transition pores [39]. The fluorescence was measured using a Multi-Mode Microplate Reader (BMG Polarstar Omega, LABTECH).

Mitochondrial function was also determined by measuring the level of ATP using the CellTiter-Glo kit, which generates a luminescent signal proportional to the amount of ATP present in the assay [40]. Cells were plated in 24-well plate at a density of 2×10^5 cells/well and after 24 h, cells were incubated with 320 μM cholesterol in the absence or in the presence of ES for 6 h. After washing, ATP levels were assayed according to manufacturer's instructions and luminescence was measured using a Multi-Mode Microplate Reader (Synergy HT, BioTek).

In addition, after 6 h-treatment with 320 μM cholesterol and/or ES, cells were incubated at 37 °C in an oxygraph apparatus equipped with a clark-type polarographic electrode (Strathkelvin Instruments dissolved oxygen respirometry systems, Warner Instruments, USA). The consumption of oxygen, which is coupled to mitochondrial respiration and ATP production was registered for 10 min. The values were normalized to the cells number.

Activities of complexes I and II of the electron transport chain were measured in mitochondria isolated from Min6 cells treated with 320 μM cholesterol in the absence or in the presence of 250 μM ES. Mitochondria were isolated as previously described previously [40]. Briefly, cells were harvested, washed in a Ca^{2+}/Mg^{2+}-free PBS and centrifuged (10 min; 1000 g; 4 °C). The pellet was resuspended and homogenized in a buffer solution (pH 7.4) containing 250 mM sucrose, 1 mM EGTA, 10 mM HEPES and 1 mg/ml BSA (fraction V). The homogenate was centrifuged (10 min; 12,000g; 4 °C); the supernatant discarded; and the pellet was washed and centrifuged as above. Complex I activity was measured in isolated mitochondria by determining the changes of $OD_{340\ nm}$ due to NADH oxidation ($\varepsilon = 6.81\ mM^{-1}\ cm^{-1}$). Rotenone (a complex I inhibitor) was used as a control; and the enzyme activity as rotenone-sensitive NADH–ubiquinone oxidoreductase was calculated [40]. The activity of complex II was quantified by the increase in 2,6-dichlorophenolindophenol (DCIP) reduction measured at 600 nm ($\varepsilon = 19.1\ mM^{-1}\ cm^{-1}$); malonate (a complex II inhibitor) was used as a control; and the enzyme activity as malonate-sensitive succinate-coenzyme Q reductase was calculated [40].

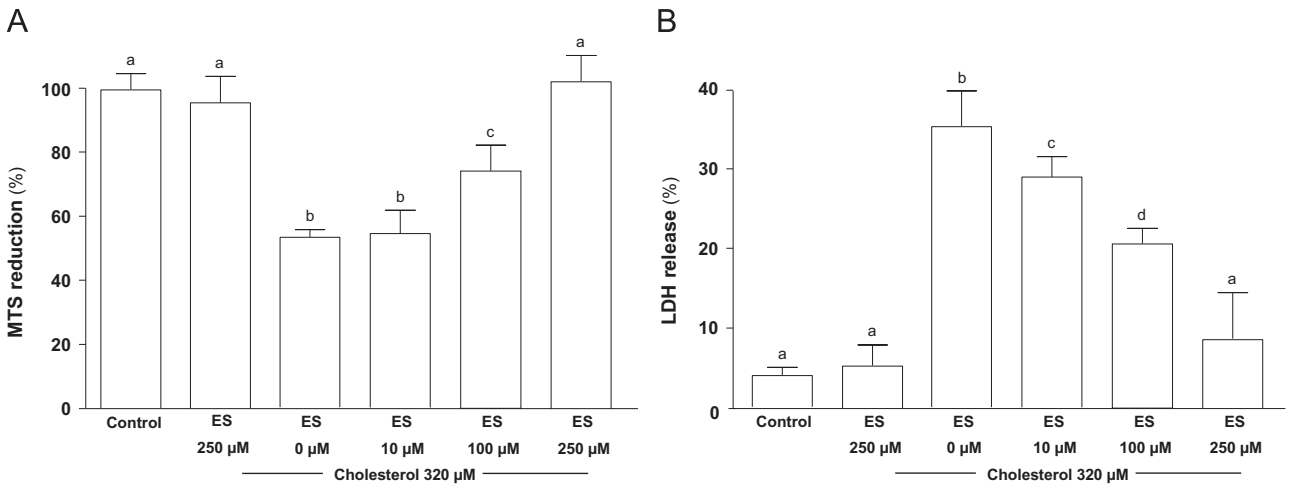

Fig. 1 – Effect of ES on the decrease of cell viability induced by cholesterol. (A) The changes in MTS reduction is expressed as percentage of the value of control (no-treated) cells, and was estimated as: ($OD_{Experimental} \times 100$)/$OD_{control\ cells}$. (B) The LDH leakage is expressed as percentage of the Triton X-100- induced maximum LDH release, and was estimated as: ($RFU_{Experimental}$ X 100)/ $RFU_{Maximum\ LDH\ release}$.

Cellular redox status assay

The redox status of Min6 cells was evaluated by measuring the intracellular reactive oxygen species and the cytosolic and mitochondrial $O_2^{\bullet -}$ production. The intracellular ROS was measured through the conversion of DCFD into a fluorescent dye (λ_{Ex} 485 nm and λ_{Em} 530 nm). $O_2^{\bullet -}$ was assessed through the specific oxidation of DHE to 2-hydroxyethidium (2-OH-E^+), also a fluorescent dye (λ_{Ex} 470 nm and λ_{Em} 590 nm) [16,41,42]. Mitochondrial $O_2^{\bullet -}$ production was evaluated through the oxidation of MitoSox™ Red, a cationic lipophilic fluorochrome (λ_{Ex} 510 nm and λ_{Em} 570 nm) which accumulates in the mitochondrial matrix [43]. Cells were plated in 24-well plates at a density of 2×10^5 cells/well and after 24 h the cells were incubated at 37 °C for 30 min with 50 μM DCFD, 10 μM DHE or 5 μM MitoSox™. After washing, cells were incubated with 320 μM cholesterol in the absence or in the presence of ES for 6 h. The fluorescence was measured using a Multi-Mode Microplate Reader (Synergy HT, BioTek).

The oxidative stress in Min6 cells was evaluated by measuring lipid peroxidation using a TBARS assay kit. Cells were plated in 75 cm^2 flask plate at a density of 2×10^7 cells and after 24 h cells were incubated with 320 μM cholesterol in the absence or in the presence of ES for 6 h. The amount of MDA in cell lysates was then quantified through the formation of a fluorescent adduct with thiobarbituric acid (λ_{Ex} 532 nm and λ_{Em} 553 nm), according to manufacturer's instructions. 1,1,3,3-tetramethoxypropane was used as control standard. The fluorescence was measured using a Multi-Mode Microplate Reader (Synergy HT, BioTek).

The antioxidant status was also assessed by measuring antioxidant enzyme activities in Min6 cells treated with 320 μM cholesterol or cholesterol plus ES. SOD determination was based on the SOD-mediated increase in the rate of autoxidation of catechols in aqueous alkaline solution to yield a chromophore with maximum absorbance at 525 nm [44]. One SOD unit was defined as the activity that doubles the auto-oxidation background and was expressed as U/mg protein. Soluble GSHpx activity was measured spectrophotometrically in the cytosolic fraction (100,000 g supernatant) by the reduction of glutathione disulfide coupled to NADPH oxidation, catalized by glutathione reductase [45]. One GSHpx unit was defined as the activity that oxidizes 1 μmol of NADPH per minute, expressed as U/mg protein.

Nrf2 activation

Nrf2 activation was evaluated by measuring the levels of Nrf2 in nuclear and cytosolic extracts, using western blotting technique. After 6 h treatment with cholesterol and/or ES, the cells were harvested and sonicated (5 s pulse, 10 pulses, 5 s between each pulse) in a buffer solution pH 7.9 containing 10 mM HEPES, 1.5 mM $MgCl_2$, 10 mM KCl, 0.2 mM PMSF, 0.5 mM DTT and 0.5% Igepal and centrifuged at 17,000*g* for 10 s. The supernatants were collected for Nrf2 quantification in the cytosolic extract. The pellets were re-suspended in a buffer solution pH 7.9 containing 20 mM HEPES, 5% Glicerol, 420 mM NaCl, 1.5 mM $MgCl_2$, 0.2 mM EDTA, 0.5 mM DTT and 0.2 mM PMSF and centrifuged at 17,000*g* for 10 min. This supernatant was collected for Nrf2 quantification in the nuclear extract. The protein content was determined in the supernatants. Protein extracts (35 μg) were resolved on a 10% SDS-PAGE, through Western blot process, and probed with rabbit polyclonal antibody for Nrf2 (1:500; 68 kDa; Abcam, Cambridge, MA) [46], lamin A/C (1:1000; 70 kDa; Cell Signaling Technology, MA) and monoclonal antibody for β-actin (1:1000; 45 kDa; Cell Signaling Technology, MA) and for α-tubulin HRP conjugated (1:1000; 52 kDa; Cell Signaling Technology, MA). In all determinations, anti-β-actin was used as control for cytosolic fractions, whereas anti-lamin A/C was used as control for nuclear fractions. In addition, the extracts were Western blotted with anti-α-tubulin or anti-lamin A/C to confirm no cross-contamination between the cytosolic and nuclear fractions, respectively. The antigen-antibody complexes were detected using horseradish peroxidase goat anti-rabbit IgG (1:2000; Cell Signaling Technology, MA) and Super Signal West Dura Extended Duration Substrate (Thermo Scientific, Rockford, IL, USA). Bands were quantified by densitometry using ImageJ.

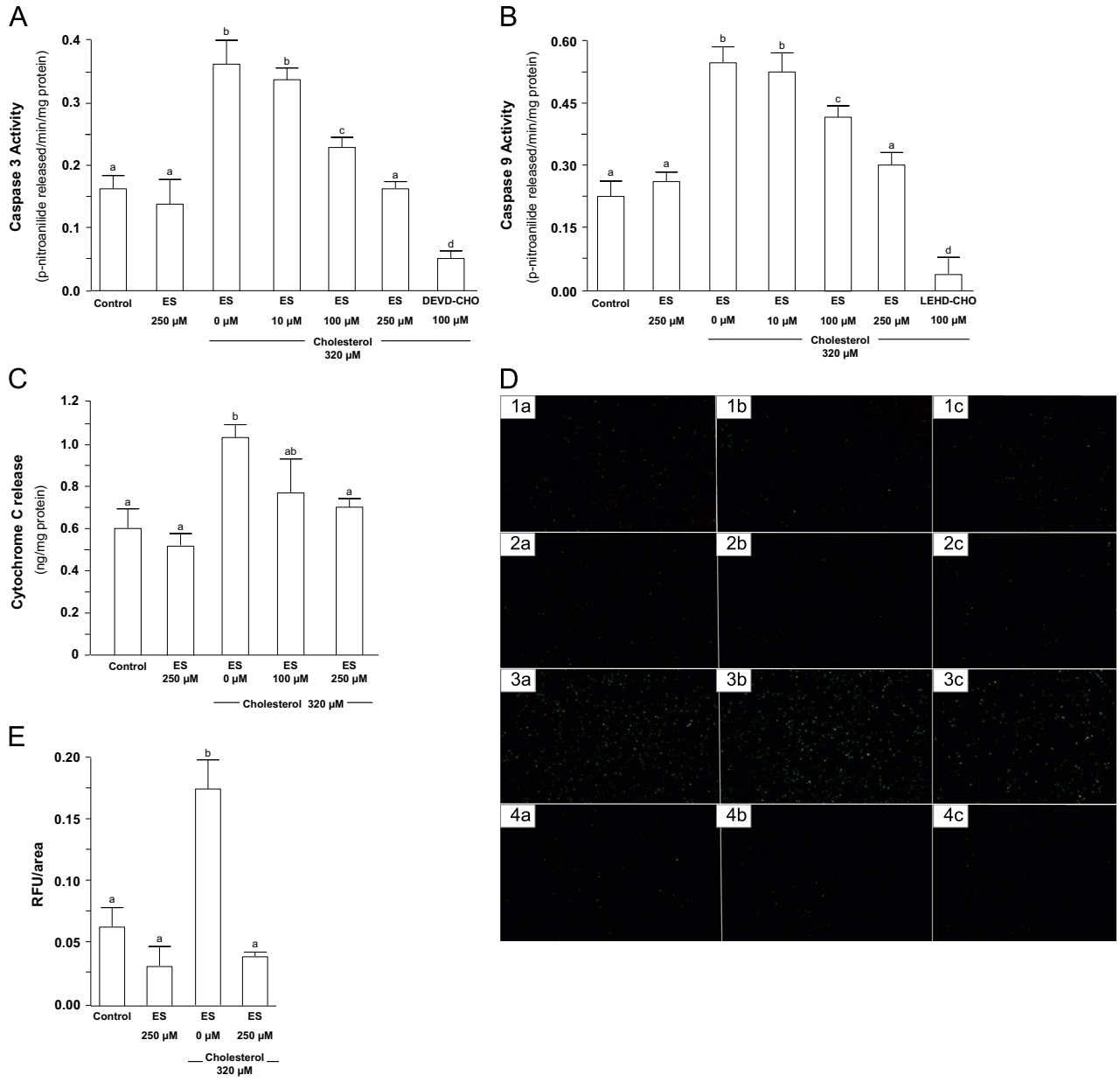

Fig. 2 – Effect of ES on apoptosis induced by cholesterol. (A) The activities of caspase-3 and (B) caspase-9 were calculated as μmol/min/mg protein. DEVD-CHO and LEHD-CHO are specific inhibitors of capase-3 and caspase-9, respectively. Enzyme activity was calculated as μmol of p-nitroanilide released/minute/mg of protein (C) Results from cytochrome c release are expressed as ng of cytochrome c/mg of protein. (D) Images of DNA fragmentation coupled to fluorescence; 1a–c) non-treated cells, 2a–c) ES-treated cells, 3a–c) cholesterol-treated cells and 4a–c) cholesterol plus ES-treated cells. (E) Quantification of DNA fragmentation.

Insulin secretion assay

It has been reported that Min6 cells with high passage (>60) numbers lose their ability to secrete insulin [47]. Min6 cells with low passage (38–41) were incubated with 320 μM cholesterol in the absence or presence of ES for 6 h, in serum-free and glucose-free DMEM supplemented with 2 mM L-glutamine and 25 mM Hepes, pH 7.4. Medium was collected for basal insulin secretion under 0 mM glucose. Cells were then washed twice with PBS and placed immediately in serum free DMEM with high glucose (25 mM) for 1 h and medium was collected for glucose-stimulated insulin secretion [47]. Insulin levels in the medium were measured by using a Rat Ultrasensitive Insulin ELISA kit, according to the manufacturer's instructions.

Statistical analysis

Data were analyzed by using the GraphPad Prism 4 statistical software throughout One-Way ANOVA, following by Tukey's post-hoc. Unless indicated otherwise, the experiments were performed three times and in quadruplicate. Values were expressed as mean ± standard deviation. Values bearing different superscript letters were significantly different ($p<0.05$).

Results

ES protects against the loss of cell viability induced by cholesterol

Exposure of cultured cells to 320 μM cholesterol decreased to 55% the capacity of reduction of MTS (Fig. 1A) and increased to 35% the leakage of LDH into the medium (Fig. 1B). Such alterations were concentration-dependently attenuated in the presence of ES. At a concentration of 250 μM, this compound totally prevented the cytotoxicity (LDH release) and the loss of cell viability (MTS assay) induced by cholesterol (Fig. 1A and B). Up to a concentration of 250 μM, ES alone did not affect cell viability.

ES protects against apoptosis induced by cholesterol

Apoptosis was studied by measuring the activation of caspases and the release of cytochrome c. Cholesterol (320 μM) treatment resulted in a 133% increase of the activities of caspase-3 and caspase-9, (Fig. 2A and B); such increases were prevented in a concentration-dependent manner in the presence of ES. ES at a concentration of 250 μM, totally prevented the increase in caspase activities (Fig. 2A and B). In addition, 320 μM cholesterol also induced an increase by 75% of the cytochrome c release and 163% of the DNA fragmentation, which was fully prevented by 250 μM of ES (Fig. 2C and D/E). Up to a concentration of 250 μM, ES alone had no effect on the markers of apoptosis.

ES protects against mitochondrial dysfunction induced by cholesterol

Cholesterol (320 μM) decreased by 40% the MMP and by 31% the intracellular levels of ATP in Min6 cells (Fig. 3A and B), in addition to decrease by 40% of the oxygen consumption rate (Fig. 3C). In the presence of ES, the cholesterol-induced mitochondrial dysfunction was concentration-dependently prevented; at 100 and 250 μM the decrease of ATP levels and MMP was totally inhibited, respectively (Fig. 3A and B). In addition, at 250 μM, the drop in oxygen consumption (Fig. 3C) and complex I activity (Fig. 3D) were completely prevented. Cholesterol had no effect on complex II activity (data not shown). Up to a concentration of 250 μM, ES alone did not affect mitochondrial function evaluated by ATP level, MMP, oxygen consumption and complexes activities.

ES protects against oxidative stress induced by cholesterol

Cholesterol (320 μM) increased by 122%, 105% and 160% the intracellular ROS, the cytosolic $O_2^{\bullet -}$ and the mitochondrial $O_2^{\bullet -}$ status, respectively (Fig. 4A, B and C). ES concentration-dependently prevented the oxidative stress induced by cholesterol. At a concentration of 100 μM, ES totally prevented the increase of intracellular ROS, since no DCF oxidation was detected. Interestingly, already at a concentration of 10 μM ES protected DHE from the oxidation induced by cholesterol, but failed in protecting against the oxidation of MitoSox™ in mitochondria. However, at 100 μM ES was able to completely prevent MitoSox™ oxidation. In addition, 320 μM cholesterol increased by 84% the basal lipid peroxidation of Min6 cells and decreased by 48% and 55% the intracellular activities of GSHpx and SOD (Fig. 4E and F), respectively. All these latter events induced by cholesterol were totally prevented by 250 μM ES. Noteworthy, ES alone increased by almost 15% the activities of GSHpx and SOD with respect to the control (Fig. 4E and F). Up to a concentration of 250 μM, ES alone had no effect on the other oxidative stress markers

ES potentiates the cholesterol-induced Nrf2 activation

Nrf2 is involved in the response to chemical/oxidative stress [48]. To assess the role of Nrf2 in the deleterious effects of cholesterol as well as in the protective effects of ES, its levels were quantified in cytosolic and nuclear extracts from Min6 cells. The purity of nuclear extraction was confirmed by its low content in α-tubulin (Fig. 4G). Cholesterol induced a 3-fold increase in nuclear *vs.* cytoplasmic Nrf2 relative to control (Fig. 4G and H). ES in the presence or absence of cholesterol increased Nrf2 translocation to the nucleus by around 6-fold relative to control ($p<0.001$, Fig. 4G and H).

ES protects against cholesterol impaired glucose-stimulated insulin secretion

Glucose (25 mM) caused a 10-fold increase in insulin secretion, in relation to non-stimulated Min6 cells (without glucose or basal secretion) (Fig. 5). Cholesterol (320 μM) decreased by 40% the insulin secretion in response to glucose, which was totally prevented in the presence of 250 μM ES (Fig. 5). ES alone, at a concentration of 250 μM, had no effect on basal or glucose-stimulated insulin secretion.

Discussion

T2DM has become a major health issue worldwide due to its high prevalence and its associated morbidity and mortality; it is currently considered one of the most challenging public health problems of the 21st century. Insulin resistance has been identified as the early key event in the pathogenesis of T2DM; pancreatic β-cell dysfunction, leading to an impaired insulin secretory response to glucose, plays a pivotal role in the transition from the pre-diabetic state to the development of clinical T2DM [1,49,50]. Cholesterol plays an important role in pancreatic β-cell dysfunction, inducing the impairment of insulin secretion [2–5,7,10]. Oxidative stress is a common pathway for numerous types of damage including glucotoxicity and lipotoxicity, and it is recognized as an important factor in pancreatic β-cell apoptosis [51]. We postulate that ES, a microbiota-derived metabolite of QUE, may protect β-pancreatic cells *in vitro* against cholesterol-induced dysfunction, and that this effect might be associated with the antioxidant and anti-apoptotic properties of this compound as well its ability to prevent mitochondrial dysfunction. This study may contribute to clarifying the possible role of ES in the systemic effects attributed to QUE *in vivo*, which are difficult to explain due to its low bioavailability.

Our results show that the viability of Min6 cells significantly decreased after 6 h of incubation with cholesterol; more specifically their ability to reduce MTS was reduced by 45%. The cholesterol concentration used in this study reflects the circulating levels observed *in vivo* since values up to 5.2 mM are considered to be in the normal range in human plasma [52].

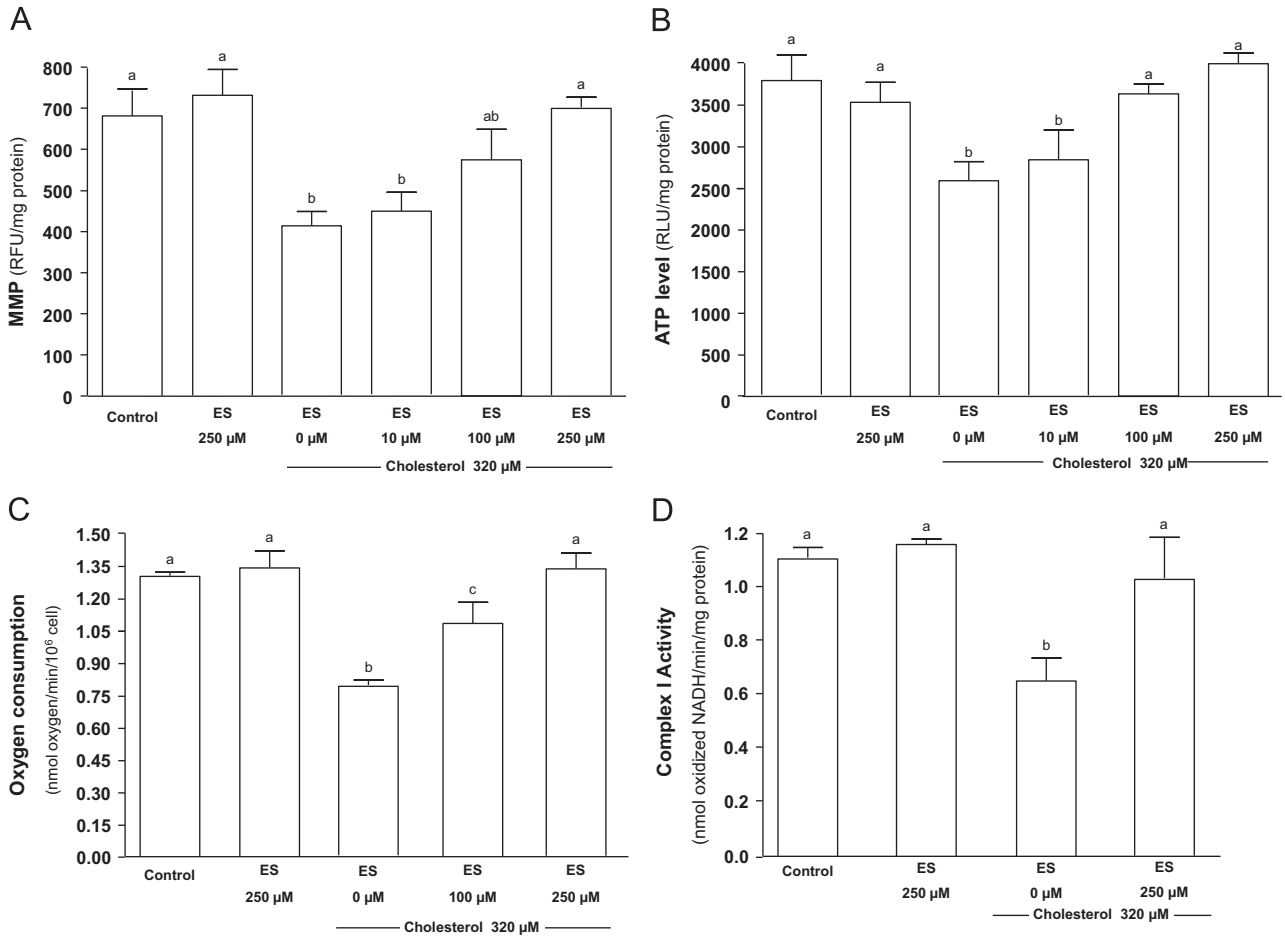

Fig. 3 – Effect of ES on mitochondrial dysfunction induced by cholesterol. (A) The MMP results are expressed as RFU/mg of protein. (B) The results of ATP levels are expressed as RLU/mg of protein. (C) The oxygen consumption results are expressed as nmol of oxygen consumed/minute/10^6 cells. (D) The activity of complex I was calculated through the rotenone-sensitive NADH oxidation and expressed as nmol of oxidized NADH/mg of protein. Values bearing different superscript letters were significantly different ($p < 0.05$).

These results confirm those of Zhao et al., who reported that cholesterol reduced the viability of Min6 cells in a concentration-dependent manner, diminishing their ability to reduce MTT [9]. In addition, this effect on cell viability was corroborated by the fact that cholesterol also induced a 35% increase in LDH leakage and trypan blue (data not shown). In line with the current study, Lu et al. reported that cholesterol decreased Min6 cell attachments to the flask bottom by 30% after 24 h of incubation [8].

In order to elucidate whether the loss of Min6 viability was due to apoptosis induction, caspase-3 and caspase-9 activity and the release of cytochrome c were assessed. Caspase-9 is an initiator caspase activated through the intrinsic (mitochondria-mediated) pathway when it is recruited by the apoptosome APAF-1/cytochrome c [53]. Caspase-9 cleaves/activates caspase-3, an effector caspase which subsequently cleaves vital cellular proteins. In the present study we observed that 6 h of incubation with cholesterol doubled the activity of caspase-3 (relative to control) (Fig. 2). This effect on caspase-3 activity was also reported by Lu et al. [8]. Zhao et al. also observed that cholesterol induced apoptosis of Min6 cells through a significant increase in phosphatidylserine on the cell surface, a phenomenon associated with cell death [9]. In addition to observing a two-fold increase in caspase-9 activity, we also detected an increase in cytochrome c release; as a result, it is possible that cholesterol induces apoptosis by activating the intrinsic pathway (Fig. 2) [36]. These findings were confirmed by the fact that the homogenates from cholesterol-treated cells were unable to exert the cleavage of caspase substrates when incubated in the presence of specific inhibitors of caspase-3 and caspase-9. The activation of effector caspases by cholesterol is consistent with an increase in DNA fragmentation in cholesterol-treated cells. These results are in line with those reported by Lu et al. with a 40% increase in DNA fragmentation after cholesterol treatment [8].

We also studied the damaging effect of cholesterol on mitochondrial function by determining the cytochrome c level as a biomarker of mitochondrial dysfunction [54]. Our results showed that cholesterol decreased the MMP, confirming the findings reported by Zhao et al. [9]. Interestingly, we also observed for the first time that cholesterol decreased ATP levels and the oxygen consumption rate (Fig. 3). It is possible that cholesterol interferes with the electron transport chain by altering the physiological efflux of protons from the mitochondrial matrix to the intermembrane space (cholesterol decreased the MMP). It also interfered with the oxygen reduction to water (cholesterol

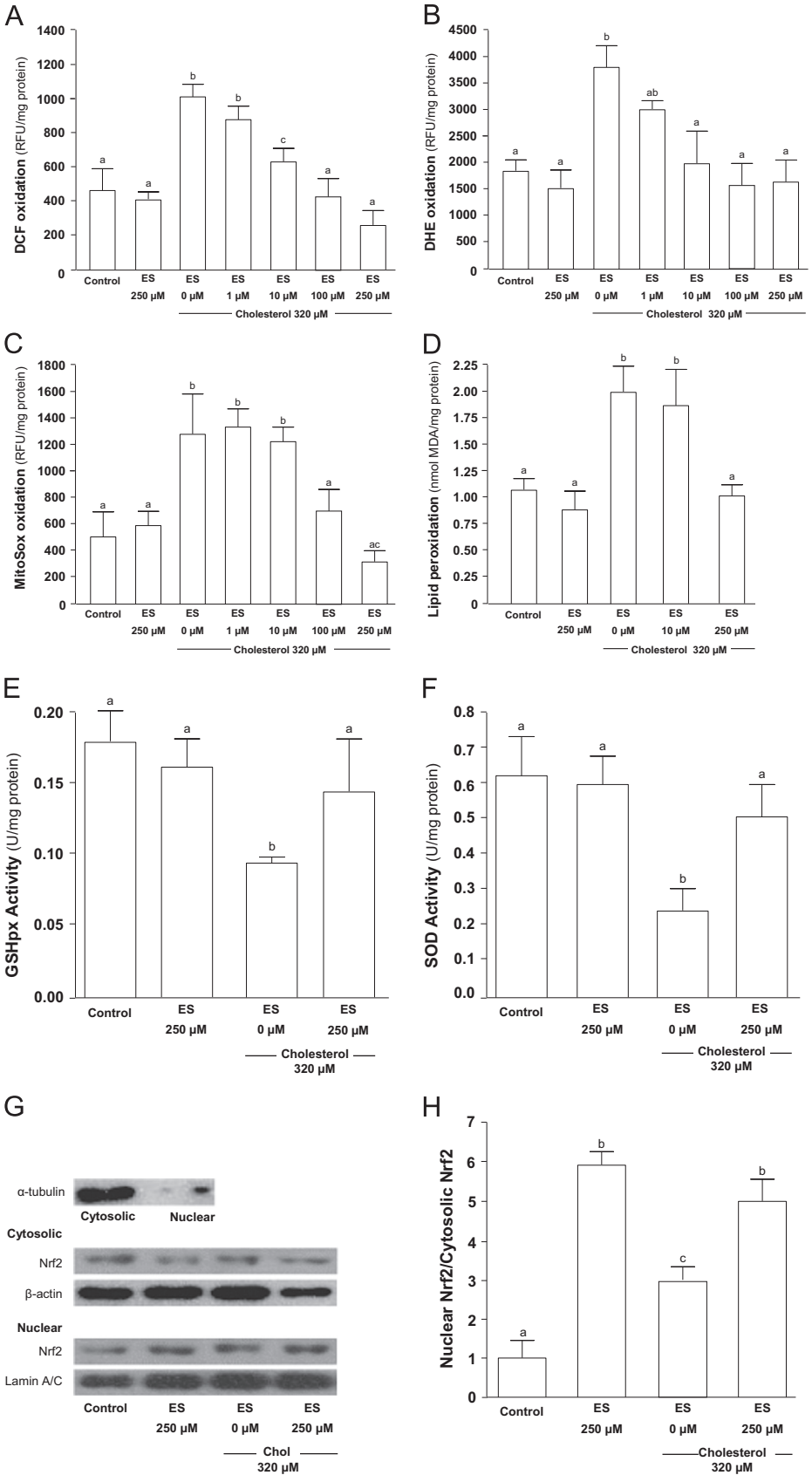

Fig. 4 – Effect of ES on oxidative stress induced by cholesterol. (A) DCF oxidation results are expressed as RFU/mg of protein. (B) DHE oxidation results are expressed as RFU/mg of protein. (C) MitoSox™ Red oxidation results are expressed as RFU/mg of protein. (D) Results from lipid peroxidation are expressed as nmol of MDA/mg of protein. (E) The activity of GSHpx and (F) SOD are expressed as U/mg protein. (G) Representative blots of nuclear and cytosolic Nrf2; β-actin, Lamin A/C and α-tubulin expression. (H) Nuclear Nrf2/Cytosolic Nrf2 content ratios and the densities of nuclear and cytosolic Nrf2 normalized by Lamin and β-actin, respectively. Chol, cholesterol. Values bearing different superscript letters were significantly different ($p<0.05$).

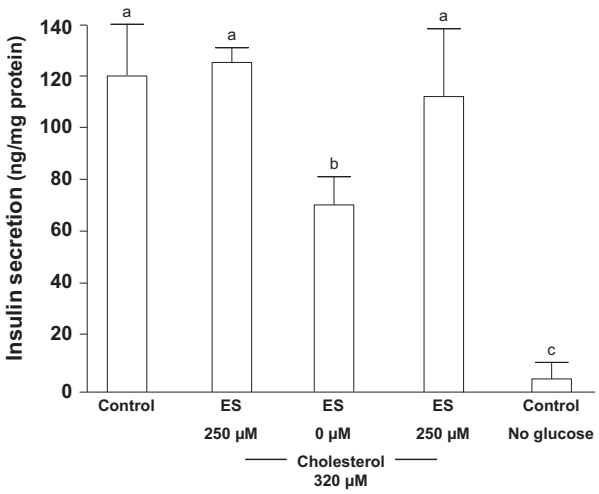

Fig. 5 – Effect of ES on impaired insulin secretion induced by cholesterol. Insulin secretion was determined in response to glucose (25 mM, for 1 h); basal insulin secretion was measured in the absence of glucose (for 6 h). Insulin secretion was assessed in the supernatant and values are expressed as ng/mg protein. Values bearing different superscript letters were significantly different ($p < 0.05$).

decreased the oxygen consumption rate). The decreased ATP levels, resulting from inadequate oxygen consumption and decreased MMP, may trigger mitochondrial swelling by inducing the permeability transition pore, a key effector of the apoptosis pathway mediated by the release of cytochrome c [54,55].

Considering that mitochondrial dysfunction is strongly associated with oxidative stress, we also evaluated the pro-oxidant effect of cholesterol. We observed that cholesterol doubled the oxidative state of Min6 cells (relative to the controls) by promoting the production of reactive oxygen species (ROS) and lipid peroxidation (Fig. 4). These observations are in line with those of Lu et al. [8], who suggested that cholesterol may induce apoptosis of β-cells by promoting oxidative stress and the activation of p38 MAPK signaling. These authors also mentioned that cholesterol induces insulin secretion impairment in Min6 cells by inducing oxidative stress and thus apoptosis. In a model of lipotoxicity using palmitate, oxidative stress mediated by NAD(P)H oxidase or uncoupled-NOS also arises as key event underlying pancreatic β-cells dysfunction [56]. Angiotensin II receptor blockers, by attenuating oxidative stress, have consistently been shown to recover decreased insulin secretion in Min6 cells and Langerhans islets isolated from mouse [57].

On the other hand, the effect of cholesterol on membrane fluidity [58] may emerge as a complementary mechanism underlying its damaging effect on pancreatic β-cells. It has recently been found that cholesterol impairs the ability of insulin secretory granules to respond to stimuli by altering membrane trafficking due to its effect on membrane rigidity, resulting in impaired insulin secretion [59]. Cholesterol accumulation in the plasma membrane has been reported to promote the formation of lipid rafts and caveolae, improving its stability and organization [60–62]. Such cholesterol-rich microdomains have been critically involved in redox-sensitive signaling events. In fact, depletion of cholesterol from membranes was reported to decrease O_2^- production by reducing the assembly of active NADPH oxidases in the cell membrane [63,64]. In addition, there may be other cholesterol-induced sources of ROS. It is worthy of note that we show, for the first time, that cholesterol induces the production of $O_2^{\bullet -}$ in mitochondria, a fact consistent with the alteration of mitochondrial function induced by this molecule (Fig. 4). The idea that cholesterol increases mitochondrial O_2^- production by inhibiting complex I is supported by the fact that rotenone and indomethacin, which inhibit complex I, also promote the mitochondrial production of $O_2^{\bullet -}$ [65,66]. Mitochondrial $O_2^{\bullet -}$ is generated by the interaction between O_2 and reducing equivalents [67]. When the electron flow through the electron transport chain slows down as well as when the H^+ builds up and the proton efflux through the inner mitochondrial membrane stops (cholesterol decreased MMP), the concentration of electron donors increases. In the absence of this gradient, the movement of H^+ through the ATP synthase ceases as does ATP formation (cholesterol decreased ATP levels). When the concentration of oxygen increases (cholesterol decreased oxygen consumption), the formation of $O_2^{\bullet -}$ by the respiratory chain also increases [67]. The rise in cholesterol-induced cytosolic $O_2^{\bullet -}$ reported in our study may be due to $O_2^{\bullet -}$ leakage from the mitochondria through the permeability transition pore and/or to $O_2^{\bullet -}$ production in the cytoplasm.

Although $O_2^{\bullet -}$ is not a strong oxidant, it is a precursor to most other ROS such as HO· (produced by the reaction between redox active metals and H_2O_2), which possess the electrical potential necessary to trigger an oxidative chain reaction (e.g. lipid peroxidation) [68]. In addition, it has been shown that $O_2^{\bullet -}$, through its auto-dismutation product, H_2O_2, may promote the inactivation of the antioxidant enzymes by oxidating their catalytic moieties [69,70]. Thus, the subsequent formation of HO· should be potentiated by the reduced activities of superoxide dismutase (SOD) and glutathione peroxidase (GSHpx). We consistently found that cholesterol, in addition to increasing the cellular $O_2^{\bullet -}$ status and decreasing antioxidant activities, also promoted lipid peroxidation. We found that cholesterol promoted Nrf2 translocation (Fig. 4H). This likely occurs via oxidative stress since cysteine residue oxidation in Keap1 induces a conformational change that disrupts the Keap1–Nrf2 association, thereby allowing Nrf2 translocation to the nucleus [71]. Interestingly, we observed that cholesterol induces the expression of antioxidant enzymes downstream from Nrf-2 activation, like HO-1, SOD and GSHpx [72]; however, these two latter became inactive due to the high pro-oxidant status of the cell (Fig. 4E and F).

Considering that insulin is a key molecule with regard to glucose homeostasis, we studied the effect of cholesterol on insulin secretion, specifically in response to glucose, due to this secretion impairment being a hallmark of the transition from pre-diabetes to diabetes. We found that cholesterol, probably by inducing oxidative stress, mitochondrial dysfunction and related apoptosis, ultimately altered the pancreatic β-cell function, impairing insulin secretion in response to glucose by 40%. Although the deleterious effect of cholesterol on insulin secretion has been previously described in Langerhans islets isolated from C57BL/6J mice and in INS-1 pancreatic β-cells, this event was addressed focusing on cholesterol interaction with the lipid raft domains within the cell membrane [4,10]. Concomitantly, since an elevation in the ATP/ADP ratio induces exocytosis of insulin triggered by a Ca^{2+} influx into the β-cell via VDCC opening induced by the ATP-sensitive K^+ channels closure-dependent

depolarization [73], the decrease in ATP levels may be a mechanism underlying the β-cell dysfunction with an impaired glucose-induced insulin secretion induced by cholesterol. In this work, we presented the cellular and mitochondrial effects of cholesterol as a new, underlying cellular mechanism to impair insulin secretion.

ES is also the major metabolite of dopamine in the central nervous system (DOPAC); therefore, most studies evaluating the cellular effect of ES have been conducted on neural cell cultures [74], and studies carried out on other types of cells are scarce. ES has been shown to exhibit a potent antiproliferative effect on colon cancer cell line HCT116 (IC_{50} 90 μM) after 24 h of incubation [75]. Skrbe et al. showed that the growth of HT29 colon cells decreased by 60% after 72 h of exposure to 100 μM ES [76]. Recently, ES synthesized by an *Aspergillus* species isolated from marine algae was shown to decrease the viability of HeLa cells at 300 μM after 24 h of incubation [77]. By contrast, in the present study ES in levels up to 250 μM had no effect on the viability of Min6 cells; however, shorter incubation times and a different cell line were used.

In the present study, ES concentration-dependently protected against cell viability loss, apoptosis, mitochondrial dysfunction and oxidative stress induced by cholesterol. Most of the protective effects were observed at a concentration of 250 μM, whereas the protection against the oxidative damage was obtained with 100 μM ES. It is possible that the protective effect of ES against lipid peroxidation and the drop in antioxidant enzyme activities may rely on its potent free radical scavenging capacities [19,23,24], preventing the oxidative attacks to lipids (Fig. 4D) and proteins and thus conserving antioxidant enzyme activities (Fig. 4E and F). The activation of Nrf2, reported here, may also contribute to the mechanism by which ES exerts its antioxidant protection, for example by increasing antioxidant enzyme activities, as suggested by the increased activities of SOD and GSHpx in ES-treated cells (without cholesterol) compared to the control cells (Fig. 4E and F). ES though Nrf2 activation may contribute to its mitochondrial protective effect, since recently Nrf2 has been proposed to be involved in mitochondrial biogenesis *via* the AMPK pathway [78]. ES may induce Nrf2 translocation to the nucleus by exerting post-translational modifications of Nrf2 via the MAPK pathway, which has been previously described for QUE [79]. However, more experiments are needed to elucidate the molecular mechanism of Nrf2 regulation by ES.

Interestingly, ES totally protected against the oxidation of an $O_2^{\bullet -}$ sensitive probe at a concentration of 10 μM when this probe was in the cytosol; however, a ten-fold higher concentration was needed when the probe was in the mitochondria. This may suggest that, unlike QUE, ES does not accumulate in mitochondria [80]; however, more specific studies are needed to establish ES distribution in cells. In addition, ES may protect against cholesterol-induced oxidative stress and mitochondrial dysfunction by preventing $O_2^{\bullet -}$ production within mitochondria by preventing the decrease of complex I activity and of mitochondrial respiration, events strongly linked to the formation mitochondrial ROS. Although it cannot be ruled out that the protective effect of ES on pancreatic β-cells could be mediated by the sequestering of cholesterol, this is unlikely since ES is highly hydrophilic and its interaction with hydrophobic compounds is questionable. By protecting against apoptosis, oxidative stress and mitochondrial dysfunction, ES should finally exert a protective effect on pancreatic β-cells and β-cell function, resulting in the prevention of the impaired glucose-stimulated insulin secretion induced by cholesterol.

With respect to the limitations of our findings, it is unlikely that ES can reach *in vivo* the effective concentration studied *in vitro* here. In fact, it is unlikely that ES is the "only" molecule responsible for the *in vivo* healthy effects attributed to QUE, but it is certainly a contributing factor. Furthermore, additional experiments are needed to establish the plasma concentrations that ES could reach in terms of a standard diet or a polyphenol-rich diet, since the available information is based mainly on studies with limited sample sizes and with subjects eating uncontrolled diets [25–27,81,82]. It should be noted that a constant urinary excretion of ES can be maintained for up to 48 h after chocolate consumption [82]. Additionally, it seems that most of the ES absorbed is metabolized to 3-methoxy-4-hydroxyphenylacetic acid, since a concentration of the methyl-derivative 24-fold higher than ES was found in the 24 h urine collections [27]. Thus, the intermediate metabolism is another important variable to consider since flavonoid bioavailability is intrinsically regulated by factors such as dietary intake, differences in host microbiota, polymorphisms of intestinal transporters, metabolic pathways and excretion, etc. Moreover, the metabolic activity of the microbiota from diabetic subjects remains to be studied, specifically in terms of polyphenol degradation.

In conclusion, this study shows for the first time the association between apoptosis, mitochondrial dysfunction and oxidative stress induced by cholesterol in Min6 cells. By inducing mitochondrial dysfunction, cholesterol could trigger oxidative stress and apoptosis. All these events ultimately cause pancreatic β-cell dysfunction with impaired insulin secretion. ES, a microbial metabolite of QUE, protects against all these damaging effects. ES is more effective in protecting cells against oxidative stress than against the other damaging effects, since lower concentrations were required for this. Nrf2 activation seems to be part of the mechanisms underlying the ES-induced antioxidant protection in addition to preventing the disruption of antioxidant enzymatic defenses. ES administration could represent a promising strategy for preventing the β-cell dysfunction induced by cholesterol *in vitro* and possibly preventing or delaying the transition from pre-diabetes to diabetes. Additional experiments are required to evaluate ES protective effects on pancreatic islets *in vivo* or *ex vivo*. In addition, given that hypercholesterolemia is associated with alterations in blood vessel differentiation and chronic cardiomyopathy, a principal cardiovascular cause of mortality linked to T2DM progression, ES could contribute to reducing the co-morbidities and mortality associated with this pathology.

Conflict of interest

Authors declare no conflict of interest.

Acknowledgments

The present study was supported by Fondecyt Initiation into Research Grant 11130232 and Australian NHMRC 0494825 and 1029178. We thank Dr. Oscar Brunser for revising the manuscript.

REFERENCES

[1] G.I. Shulman, Cellular mechanisms of insulin resistance, J. Clin. Investig. 106 (2000) 171–176.

[2] L.R. Brunham, J.K. Kruit, T.D. Pape, J.M. Timmins, A.Q. Reuwer, Z. Vasanji, B.J. Marsh, B. Rodrigues, J.D. Johnson, J.S. Parks, C.B. Verchere, M.R. Hayden, Beta-cell ABCA1 influences insulin secretion, glucose homeostasis and response to thiazolidinedione treatment, Nat. Med. 13 (2007) 340–347.

[3] I. Gerin, V.W. Dolinsky, J.G. Shackman, R.T. Kennedy, S.H. Chiang, C.F. Burant, K.R. Steffensen, J.A. Gustafsson, O.A. MacDougald, LXRbeta is required for adipocyte growth, glucose homeostasis, and beta cell function, J. Biol. Chem. 280 (2005) 23024–23031.

[4] M. Hao, W.S. Head, S.C. Gunawardana, A.H. Hasty, D.W. Piston, Direct effect of cholesterol on insulin secretion: a novel mechanism for pancreatic beta-cell dysfunction, Diabetes 56 (2007) 2328–2338.

[5] M.L. Bonfleur, E.C. Vanzela, R.A. Ribeiro, G. de Gabriel Dorighello, C.P. de Franca Carvalho, C.B. Collares-Buzato, E.M. Carneiro, A.C. Boschero, H.C. de Oliveira, Primary hypercholesterolaemia impairs glucose homeostasis and insulin secretion in low-density lipoprotein receptor knockout mice independently of high-fat diet and obesity, Biochim. Biophys. Acta 2010 (1801) 183–190.

[6] J.M. Sturek, J.D. Castle, A.P. Trace, L.C. Page, A.M. Castle, C. Evans-Molina, J.S. Parks, R.G. Mirmira, C.C. Hedrick, An intracellular role for ABCG1-mediated cholesterol transport in the regulated secretory pathway of mouse pancreatic Î² cells, J. Clin Invest. 120 (2010) 2575–2589.

[7] M. Ishikawa, Y. Iwasaki, S. Yatoh, T. Kato, S. Kumadaki, N. Inoue, T. Yamamoto, T. Matsuzaka, Y. Nakagawa, N. Yahagi, K. Kobayashi, A. Takahashi, N. Yamada, H. Shimano, Cholesterol accumulation and diabetes in pancreatic beta-cell-specific SREBP-2 transgenic mice: a new model for lipotoxicity, J. Lipid Res. 49 (2008) 2524–2534.

[8] X. Lu, J. Liu, F. Hou, Z. Liu, X. Cao, H. Seo, B. Gao, Cholesterol induces pancreatic beta cell apoptosis through oxidative stress pathway, Cell Stress Chaperones 16 (2011) 539–548.

[9] Y.F. Zhao, L. Wang, S. Lee, Q. Sun, Y. Tuo, Y. Wang, J. Pei, C. Chen, Cholesterol induces mitochondrial dysfunction and apoptosis in mouse pancreatic beta-cell line MIN6 cells, Endocrine 37 (2010) 76–82.

[10] R. Dirkx Jr, M. Solimena, Cholesterol-enriched membrane rafts and insulin secretion, J. Diabetes Investig. 3 (2012) 339–346.

[11] K. Grankvist, S.L. Marklund, I.B. Taljedal, CuZn-superoxide dismutase, Mn-superoxide dismutase, catalase and glutathione peroxidase in pancreatic islets and other tissues in the mouse, Biochem. J. 199 (1981) 393–398.

[12] G.S. Kelly, Quercetin monograph, Altern. Med. Rev. 16 (2011) 172–194.

[13] X. Cai, Z. Fang, J. Dou, A. Yu, G. Zhai, Bioavailability of quercetin: problems and promises, Curr. Med. Chem. 20 (2013) 2572–2582.

[14] J.M. Landete, Updated knowledge about polyphenols: functions, bioavailability, metabolism, and health, Crit. Rev. Food Sci. Nutr. 52 (2012) 936–948.

[15] A.M. Aura, K.A. O'Leary, G. Williamson, M. Ojala, M. Bailey, R. Puupponen-Pimia, A.M. Nuutila, K.M. Oksman-Caldentey, K. Poutanen, Quercetin derivatives are deconjugated and converted to hydroxyphenylacetic acids but not methylated by human fecal flora *in vitro*, J. Agric. Food Chem. 50 (2002) 1725–1730.

[16] L. Benov, L. Sztejnberg, I. Fridovich, Critical evaluation of the use of hydroethidine as a measure of superoxide anion radical, Free Radic. Biol. Med. 25 (1998) 826–831.

[17] M. Blaut, L. Schoefer, A. Braune, Transformation of flavonoids by intestinal microorganisms, Int. J. Vitam. Nutr. Res. 73 (2003) 79–87.

[18] A. Braune, M. Gutschow, W. Engst, M. Blaut, Degradation of quercetin and luteolin by *Eubacterium ramulus*, Appl. Environ. Microbiol. 67 (2001) 5558–5567.

[19] L.M. LeBlanc, A.F. Pare, J. Jean-Francois, M.J. Hebert, M.E. Surette, M. Touaibia, Synthesis and antiradical/antioxidant activities of caffeic acid phenethyl ester and its related propionic, acetic, and benzoic acid analogues, Molecules 17 (2012) 14637–14650.

[20] C. Manach, G. Williamson, C. Morand, A. Scalbert, C. Remesy, Bioavailability and bioefficacy of polyphenols in humans. I. Review of 97 bioavailability studies, Am. J. Clin. Nutr. 81 (2005) 230–242.

[21] H. Schneider, A. Schwiertz, M.D. Collins, M. Blaut, Anaerobic transformation of quercetin-3-glucoside by bacteria from the human intestinal tract, Arch. Microbiol. 171 (1999) 81–91.

[22] L. Schoefer, R. Mohan, A. Schwiertz, A. Braune, M. Blaut, Anaerobic degradation of flavonoids by Clostridium orbiscindens, Appl. Environ. Microbiol. 69 (2003) 5849–5854.

[23] V. Raneva, H. Shimasaki, Y. Ishida, N. Ueta, E. Niki, Antioxidative activity of 3,4-dihydroxyphenylacetic acid and caffeic acid in rat plasma, Lipids 36 (2001) 1111–1116.

[24] C.A. Rice-Evans, N.J. Miller, G. Paganga, Structure-antioxidant activity relationships of flavonoids and phenolic acids, Free Radic. Biol. Med. 20 (1996) 933–956.

[25] M. Gross, M. Pfeiffer, M. Martini, D. Campbell, J. Slavin, J. Potter, The quantitation of metabolites of quercetin flavonols in human urine, Cancer Epidemiol. Biomarkers Prev. 5 (1996) 711–720.

[26] M.R. Olthof, P.C. Hollman, M.N. Buijsman, J.M. van Amelsvoort, M.B. Katan, Chlorogenic acid, quercetin-3-rutinoside and black tea phenols are extensively metabolized in humans, J. Nutr. 133 (2003) 1806–1814.

[27] M. Urpi-Sarda, M. Monagas, N. Khan, R. Llorach, R.M. Lamuela-Raventos, O. Jauregui, R. Estruch, M. Izquierdo-Pulido, C. Andres-Lacueva, Targeted metabolic profiling of phenolics in urine and plasma after regular consumption of cocoa by liquid chromatography-tandem mass spectrometry, J. Chromatogr. A 1216 (2009) 7258–7267.

[28] O. Coskun, M. Kanter, A. Korkmaz, S. Oter, Quercetin, a flavonoid antioxidant, prevents and protects streptozotocin-induced oxidative stress and beta-cell damage in rat pancreas, Pharmacol. Res. 51 (2005) 117–123.

[29] T.M. Henagan, N.R. Lenard, T.W. Gettys, L.K. Stewart, Dietary quercetin supplementation in mice increases skeletal muscle pgc1alpha expression, improves mitochondrial function and attenuates insulin resistance in a time-specific manner, PLoS One 9 (2014) e89365.

[30] S.M. Jeong, M.J. Kang, H.N. Choi, J.H. Kim, J.I. Kim, Quercetin ameliorates hyperglycemia and dyslipidemia and improves antioxidant status in type 2 diabetic db/db mice, Nutr. Res. Pract. 6 (2012) 201–207.

[31] J.M. Li, W. Wang, C.Y. Fan, M.X. Wang, X. Zhang, Q.H. Hu, L.D. Kong, Quercetin preserves beta -cell mass and function in fructose-induced hyperinsulinemia through modulating pancreatic Akt/FoxO1 activation, Evid. Based Complement. Altern. Med. 2013 (2013) 303902.

[32] C.-H. Lai, Y.-C. Chang, S.-Y. Du, H.-J. Wang, C.-H. Kuo, S.-H. Fang, H.-W. Fu, H.-H. Lin, A.-S. Chiang, W.-C. Wang, Cholesterol depletion reduces Helicobacter pylori CagA translocation and CagA-induced responses in AGS cells, Infect. Immun. 76 (2008) 3293–3303.

[33] N. Khatibzadeh, A.A. Spector, W.E. Brownell, B. Anvari, Effects of Plasma Membrane Cholesterol Level and Cytoskeleton F-Actin on Cell Protrusion Mechanics, PLoS One 8 (2013) e57147.

[34] W. Ziolkowski, M. Szkatula, A. Nurczyk, T. Wakabayashi, J.J. Kaczor, R.A. Olek, N. Knap, J. Antosiewicz, M.R. Wieckowski, M. Wozniak, Methyl-beta-cyclodextrin induces mitochondrial cholesterol depletion and alters the mitochondrial structure and bioenergetics, FEBS Letters 584 4606-4610.

[35] C. Carrasco-Pozo, E. Pastene, C. Vergara, M. Zapata, C. Sandoval, M. Gotteland, Stimulation of cytosolic and mitochondrial calcium mobilization by indomethacin in Caco-2 cells: modulation by the

polyphenols quercetin, resveratrol and rutin, Biochim. Biophys. Acta 2012 (1820) 2052–2061.
[36] X. Jiang, X. Wang, Cytochrome C-mediated apoptosis, Annu. Rev. Biochem. 73 (2004) 87–106.
[37] X. Li, W. Wen, K. Liu, F. Zhu, M. Malakhova, C. Peng, T. Li, H.G. Kim, W. Ma, Y.Y. Cho, A.M. Bode, Z. Dong, Phosphorylation of caspase-7 by p21-activated protein kinase (PAK) 2 inhibits chemotherapeutic drug-induced apoptosis of breast cancer cell lines, J. Biol. Chem. 286 (2011) 22291–22299.
[38] J.G. Walsh, S.P. Cullen, C. Sheridan, A.U. Luthi, C. Gerner, S.J. Martin, Executioner caspase-3 and caspase-7 are functionally distinct proteases, Proc. Natl. Acad. Sci. USA 105 (2008) 12815–12819.
[39] C. Zazueta, H. Reyes-Vivas, C. Bravo, J. Pichardo, N. Corona, E. Chavez, Triphenyltin as inductor of mitochondrial membrane permeability transition, J. Bioenerg. Biomembr. 26 (1994) 457–462.
[40] C. Carrasco-Pozo, M.L. Mizgier, H. Speisky, M. Gotteland, Differential protective effects of quercetin, resveratrol, rutin and epigallocatechin gallate against mitochondrial dysfunction induced by indomethacin in Caco-2 cells, Chem. Biol. Interact. 195 (2012) 199–205.
[41] J. Zielonka, J. Vasquez-Vivar, B. Kalyanaraman, The confounding effects of light, sonication, and Mn(III)TBAP on quantitation of superoxide using hydroethidine, Free Radic. Biol. Med. 41 (2006) 1050–1057.
[42] H. Zhao, J. Joseph, H.M. Fales, E.A. Sokoloski, R.L. Levine, J. Vasquez-Vivar, B. Kalyanaraman, Detection and characterization of the product of hydroethidine and intracellular superoxide by HPLC and limitations of fluorescence, Proc. Natl. Acad. Sci. USA 102 (2005) 5727–5732.
[43] Y. Li, D.F. Boehning, T. Qian, V.L. Popov, S.A. Weinman, Hepatitis C virus core protein increases mitochondrial ROS production by stimulation of Ca2+ uniporter activity, FASEB J. 21 (2007) 2474–2485.
[44] C. Nebot, M. Moutet, P. Huet, J.Z. Xu, J.C. Yadan, J. Chaudiere, Spectrophotometric assay of superoxide dismutase activity based on the activated autoxidation of a tetracyclic catechol, Anal. Biochem. 214 (1993) 442–451.
[45] L. Flohe, W.A. Gunzler, Assays of glutathione peroxidase, Methods Enzymol. 105 (1984) 114–121.
[46] P. Romanque, P. Cornejo, S. Valdes, L.A. Videla, Thyroid hormone administration induces rat liver Nrf2 activation: suppression by N-acetylcysteine pretreatment, Thyroid 21 (2011) 655–662.
[47] K. Cheng, V. Delghingaro-Augusto, C.J. Nolan, N. Turner, N. Hallahan, S. Andrikopoulos, J.E. Gunton, High passage MIN6 cells have impaired insulin secretion with impaired glucose and lipid oxidation, PLoS One 7 (7) (2012) e40868 doi: 10.1371/journal.pone.0040868. Epub 2012 Jul 13.
[48] A.L. Eggler, K.A. Gay, A.D. Mesecar, Molecular mechanisms of natural products in chemoprevention: induction of cytoprotective enzymes by Nrf2, Mol. Nutr. Food Res. 52 (2008) 200700249.
[49] V. Lyssenko, P. Almgren, D. Anevski, R. Perfekt, K. Lahti, M. Nissen, B. Isomaa, B. Forsen, N. Homstrom, C. Saloranta, M.R. Taskinen, L. Groop, T. Tuomi, Predictors of and longitudinal changes in insulin sensitivity and secretion preceding onset of type 2 diabetes, Diabetes 54 (2005) 166–174.
[50] A.G. Tabak, C. Herder, W. Rathmann, E.J. Brunner, M. Kivimaki, Prediabetes: a high-risk state for diabetes development, Lancet 379 (2012) 2279–2290.
[51] Z. Li, Z. Zhou, G. Huang, F. Hu, Y. Xiang, L. He, Exendin-4 protects mitochondria from reactive oxygen species induced apoptosis in pancreatic Beta cells, PLoS One 8 (2013).
[52] M. Rauchhaus, A.L. Clark, W. Doehner, C. Davos, A. Bolger, R. Sharma, A.J. Coats, S.D. Anker, The relationship between cholesterol and survival in patients with chronic heart failure, J. Am. Coll. Cardiol. 42 (2003) 1933–1940.
[53] D. Twiddy, K. Cain, Caspase-9 cleavage, do you need it?#, Biochem. J. 405 (2007) e1–2.
[54] E. Latz, T.S. Xiao, A. Stutz, Activation and regulation of the inflammasomes, Nat. Rev. Immunol. 13 (2013) 397–411.
[55] V. Giorgio, S. von Stockum, M. Antoniel, A. Fabbro, F. Fogolari, M. Forte, G.D. Glick, V. Petronilli, M. Zoratti, I. Szabo, G. Lippe, P. Bernardi, Dimers of mitochondrial ATP synthase form the permeability transition pore, Proc. Natl. Acad. Sci. USA 110 (2013) 5887–5892.
[56] T. Inoguchi, H. Nawata, NAD(P)H oxidase activation: a potential target mechanism for diabetic vascular complications, progressive beta-cell dysfunction and metabolic syndrome, Curr. Drug Targets 6 (2005) 495–501.
[57] Y. Saitoh, W. Hongwei, H. Ueno, M. Mizuta, M. Nakazato, Candesartan attenuates fatty acid-induced oxidative stress and NAD(P)H oxidase activity in pancreatic beta-cells, Diabetes Res. Clin. Pract. 90 (2010) 54–59.
[58] L. Liscum, Niemann-Pick type C mutations cause lipid traffic jam, Traffic 1 (2000) 218–225.
[59] J.S. Bogan, Y. Xu, M. Hao, Cholesterol accumulation increases insulin granule size and impairs membrane trafficking, Traffic 13 (2012) 1466–1480.
[60] J.R. Silvius, Role of cholesterol in lipid raft formation: lessons from lipid model systems, Biochim. Biophys. Acta 10 (2003) 174–183.
[61] K. Gaus, E. Gratton, E.P. Kable, A.S. Jones, I. Gelissen, L. Kritharides, W. Jessup, Visualizing lipid structure and raft domains in living cells with two-photon microscopy, Proc. Natl. Acad. Sci. USA 100 (2003) 15554–15559.
[62] A.Y. Zhang, F. Yi, G. Zhang, E. Gulbins, P.L. Li, Lipid raft clustering and redox signaling platform formation in coronary arterial endothelial cells, Hypertension 47 (2006) 74–80.
[63] E.J. Henriksen, M.K. Diamond-Stanic, E.M. Marchionne, Oxidative stress and the etiology of insulin resistance and type 2 diabetes, Free Radic. Biol. Med. 51 (2011) 993–999.
[64] S. Jin, F. Zhou, F. Katirai, P.L. Li, Lipid raft redox signaling: molecular mechanisms in health and disease, Antioxid. Redox Signal. 15 (2011) 1043–1083.
[65] M.P. Murphy, How mitochondria produce reactive oxygen species, Biochem. J. 417 (2009) 1–13.
[66] C. Carrasco-Pozo, M. Gotteland, H. Speisky, Apple peel polyphenol extract protects against indomethacin-induced damage in Caco-2 cells by preventing mitochondrial complex I inhibition, J. Agric. Food. Chem. 59 (2011) 11501–11508.
[67] J.F. Turrens, Mitochondrial formation of reactive oxygen species, J. Physiol. 552 (2003) 335–344.
[68] J.M. Gutteridge, D.A. Rowley, B. Halliwell, Superoxide-dependent formation of hydroxyl radicals and lipid peroxidation in the presence of iron salts. Detection of 'catalytic' iron and antioxidant activity in extracellular fluids, Biochem. J. 206 (1982) 605–609.
[69] E. Pigeolet, J. Remacle, Susceptibility of glutathione peroxidase to proteolysis after oxidative alteration by peroxides and hydroxyl radicals, Free Radic. Biol. Med. 11 (1991) 191–195.
[70] E.K. Hodgson, I. Fridovich, The interaction of bovine erythrocyte superoxide dismutase with hydrogen peroxide: inactivation of the enzyme, Biochemistry 14 (1975) 5294–5299.
[71] H.K. Bryan, A. Olayanju, C.E. Goldring, B.K. Park, The Nrf2 cell defence pathway: keap1-dependent and -independent mechanisms of regulation, Biochem. Pharmacol. 85 (2013) 705–717.
[72] C. Carrasco-Pozo, K.N. Tan, S.T. Ngo and K. Borges, Quercetin protects against cholesterol-induced pancreatic β-cell dysfunction: role of SIRT1, PGC-1alpha, Nrf2- and NFkB-pathways Submitted 2015.
[73] J.C. Koster, M.A. Permutt, C.G. Nichols, Diabetes and insulin secretion: the ATP-sensitive K+ channel (KATP) connection, Diabetes 54 (2005) 3065–3072.
[74] I.J. Kopin, Catecholamine metabolism: basic aspects and clinical significance, Pharmacol. Rev. 37 (1985) 333–364.

[75] K. Gao, A. Xu, C. Krul, K. Venema, Y. Liu, Y. Niu, J. Lu, L. Bensoussan, N.P. Seeram, D. Heber, S.M. Henning, Of the major phenolic acids formed during human microbial fermentation of tea, citrus, and soy flavonoid supplements, only 3,4-dihydroxyphenylacetic acid has antiproliferative activity, J. Nutr. 136 (2006) 52–57.
[76] S. Skrbek, C.E. Rufer, D. Marko, M. Esselen, Quercetin and its microbial degradation product 3,4-dihydroxyphenylacetic acid generate hydrogen peroxide modulating their stability under *in vitro* conditions, J. Food Nutr. Res. 48 (2009) 129–140.
[77] M.J. Jo, S.J. Bae, B.W. Son, C.Y. Kim, G.D. Kim, 3,4-dihydroxyphenyl acetic acid and (+)-epoxydon isolated from marine algae-derived microorganisms induce down regulation of epidermal growth factor activated mitogenic signaling cascade in Hela cells, Cancer Cell Int. 13 (2013) 49.
[78] M.L. Pall, S. Levine, Nrf2, a master regulator of detoxification and also antioxidant, anti-inflammatory and other cytoprotective mechanisms, is raised by health promoting factors, Sheng Li Xue Bao 67 (2015) 1–18.
[79] A.B. Granado-Serrano, M.A. Martin, L. Bravo, L. Goya, S. Ramos, Quercetin modulates Nrf2 and glutathione-related defenses in HepG2 cells: involvement of p38, Chem. Biol. Interact. 195 (2012) 154–164.
[80] M. Fiorani, A. Guidarelli, M. Blasa, C. Azzolini, M. Candiracci, E. Piatti, O. Cantoni, Mitochondria accumulate large amounts of quercetin: prevention of mitochondrial damage and release upon oxidation of the extramitochondrial fraction of the flavonoid, J. Nutr. Biochem. 21 (2010) 397–404.
[81] A.M. Jenner, J. Rafter, B. Halliwell, Human fecal water content of phenolics: the extent of colonic exposure to aromatic compounds, Free Radic. Biol. Med. 38 (2005) 763–772.
[82] L.Y. Rios, M.P. Gonthier, C. Remesy, I. Mila, C. Lapierre, S.A. Lazarus, G. Williamson, A. Scalbert, Chocolate intake increases urinary excretion of polyphenol-derived phenolic acids in healthy human subjects, Am. J. Clin. Nutr. 77 (2003) 912–918.

Glossary

ABCA1: ATP-binding cassette transporter subfamily A member 1
DCFD: 2′,7′-dichlorofluorescein diacetate
DHE: dihydroethidium
ES: 3,4 dihydroxyphenylacetic acid
GSHpx: glutathione peroxidase
LDH: lactate dehydrogenase
MDA: malondialdehyde
MMP: Mitochondrial membrane potential
MTS: (3-(4,5-dimethylthiazol-2-yl)-5-(3-carboxymethoxyphenyl)-2-(4-sulfophenyl)-2H-tetrazolium)
MTT: 3-(4,5-dimethylthiazol-2-yl)-2,5-diphenyltetrazolium bromide
Nrf2: Nuclear factor (erythroid-derived 2)-like 2
Rhod: rhodamine 123
RFU: relative fluorescence unit
RLU: relative luminescence unit
$O_2^{\cdot-}$: superoxide anion radicals
QUE: quercetin
ROS: reactive oxygen species
SOD: superoxide dismutase
TEAC: Trolox equivalent antioxidant activity
T2DM: type 2 diabetes mellitus
TBARS: Thiobarbituric acid reactive substances.